AIAA Aviation
22-26 June 2015, Dallas, TX
22nd AIAA Computational Fluid Dynamics Conference

Opportunities for efficient high-order methods based on the summation-by-parts property

Jason E. Hicken*, a David C. Del Rey Fernández†, b
David W. Zingg‡, b
Rensselaer Polytechnic Institute[a]
University of Toronto Institute for Aerospace Studies[b]

Summation-by-parts (SBP) operators are traditionally viewed as high-order finite-difference operators, but they can also be interpreted as finite-element operators with an implicit basis. Such an element-based perspective leads to several opportunities that we describe. The first is provided by generalized one-dimensional SBP operators, which maintain the desirable properties of classical SBP operators while permitting flexible nodal distributions. The second opportunity is to extend the SBP definition to multiple dimensions, and a recently proposed definition for multidimensional SBP operators paves the way for time-stable, high-order finite-difference operators on unstructured grids. The final opportunity that we discuss is an analogy with the continuous Galerkin finite-element method, which leads to a systematic means of assembling SBP operators on a global domain from elemental operators. To illustrate these ideas, high-order SBP operators are constructed for the triangle and tetrahedron, and the former are assembled into a global SBP operator and applied to a linear convection problem on a triangular grid.

I. Introduction

The potential efficiency of high-order methods in the numerical solution of partial differential equations has been recognized since the seminal work of Kreiss and Oliger [1] and Swartz and Wendroff [2]. A large variety of high-order methods have been proposed, including but not limited to finite-difference, finite-element, finite-volume, spectral-difference, spectral-element, and spectral-volume methods. Within each category there exist several different approaches as well. Recently the discontinuous Galerkin and flux reconstruction methods have drawn considerable interest. The recent high-order workshops provide a snapshot of some high-order approaches of current interest [3].

The interest in high-order methods is often limited to simulations of turbulent flows, aeroacoustics, wave propagation problems, and other time-dependent flows. However, the basic advantage of high-order methods is not restricted to time-dependent problems, and such methods have the potential to be beneficial in the computation of steady flows governed by the Reynolds-averaged Navier-Stokes (RANS) equations as well [4]. An important point is that the benefit of a high-order method over a second-order method increases as the numerical accuracy requirement becomes more stringent. Therefore one can argue that, given that turbulence modeling and transition prediction can introduce significant error, one often does not have a particularly stringent numerical accuracy requirement when solving the steady RANS equations. However, there are conditions, e.g. cruise conditions for an aircraft, where turbulence modeling errors are small and grid density requirements for appropriate numerical accuracy are high. In these cases, a high-order method may well be advantageous in providing equivalent numerical accuracy at a lower cost than a second-order method.

For many problems of interest, high-order methods cannot achieve their design order due to singularities such as an airfoil trailing edge or discontinuities such as shock waves. Even under these conditions high-order

*Assistant Professor
†Ph.D. candidate, Institute for Aerospace Studies, 4925 Dufferin St., and AIAA Student Member (dcdelrey@gmail.com)
‡Professor and Director, J. Armand Bombardier Foundation Chair in Aerospace Flight, Institute for Aerospace Studies, 4925 Dufferin St., and AIAA Member Grade.

methods can nevertheless show efficiency benefits as a result of their accuracy in smooth regions of the flow. Adaptive methods provide a complementary means of improving efficiency. Either the method or the grid can be adaptively altered based on the solution. Such approaches are particularly powerful when a functional is of interest and adjoint variables are used to determine the impact of the local discretization error on the accuracy of the functional.

Given the wide variety of methods available, it is of interest to understand and quantify the trade-offs associated with various approaches in the context of popular problem classes. For example, for reasonably smooth geometries, it is possible to generate a smooth mesh and therefore a smooth coordinate transformation in order to enable the application of a finite-difference method extended to multiple dimensions through Kronecker products, which can be very efficient. However, this approach becomes less effective with increasing geometric complexity such that it becomes difficult to find a sufficiently smooth coordinate transformation. For such problems, unstructured grids are appealing, in particular methods that do not rely on mesh smoothness, i.e. those with interior degrees of freedom. Unstructured grids are often better suited to solution adaptation as well.

For the purpose of this paper, we will consider operators that can be divided into two classes. The first class is associated with the traditional implementation of finite-difference methods in which the operator in the interior of the domain is the same for all nodes and there are a finite number of boundary operators. The second class is associated with finite-element methods, where each element has an associated operator and the elements are coupled in some manner. In the first class of methods the mesh is refined by increasing the number of grid nodes, which in turn increases the number of nodes where the interior operator is applied. In the element approach, increased resolution can be achieved either by increasing the number of elements (h refinement), by raising the order of the operators by increasing the number of interior degrees of freedom (p refinement), or both (hp refinement).

One of the observations in this paper is that methods normally considered to be finite-difference methods can be applied in an element type manner. One often defines finite-difference methods in terms of two properties. First, they are derived on the basis of Taylor series expansions [5]. Second, they involve a repeating interior operator. Here we will consider only the first property to be the defining characteristic of a finite-difference method. Thus we will consider any matrix operator for which the entries of the matrix are derived through a Taylor series analysis or equivalent to be a finite-difference operator. In particular this contrasts with the use of basis functions in the finite-element method. This perspective opens up some useful avenues to derive new methods with excellent properties. Such ideas are not new. There are many methods, for example some meshless methods, that are difficult to classify and blur the distinction between finite-difference and finite-element methods. An interesting recent example can be found in Ditkowski [6], where he introduces finite-difference operators with two- and three-point blocks.

A primary challenge in deriving high-order finite-difference methods is to ensure their stability. Typically this involves finding boundary operators that can be used in conjunction with a selected interior operator to produce a stable scheme[a] with global accuracy as close as possible to that associated with the interior operator. Summation by parts (SBP) operators provide an excellent mechanism to construct provably stable high-order finite-difference methods [7–10]. Typically used with a weak imposition of boundary conditions through penalty terms (simultaneous approximation terms or SATs [11–13]), SBP methods are strongly associated with finite-difference methods implemented in the traditional manner with a repeating interior operator, as described above. However, Carpenter and Gottlieb [14], Gassner [15], and others have shown that other known operators possess the SBP property. Del Rey Fernández *et al.* [16] showed that the SBP concept can be extended from the classical operators on a uniform nodal distribution implemented in the traditional manner to include operators that involve a nonuniform nodal distribution (which need not include boundary nodes) and are not characterized by a repeating interior operator. This generalization leads to both operators that can be implemented either in the traditional finite-difference manner or as elements and operators that can only be implemented as elements. This is discussed further in Section II B.

Together the concept of a generalized SBP operator and the idea of implementing SBP operators as elements provide a basis for the development of SBP operators in multiple dimensions applicable to unstructured grids. This provides a very general approach to the construction of stable operators for such grids with the potential to lead to novel operators with useful properties. The objective of this paper is to present an approach to the construction of SBP operators in multiple dimensions and to provide some examples of operators that can be constructed within the wide class of possible operators.

[a]We will discuss only time stability here.

In the next section we provide a quick introduction to the SBP property. This is followed by a discussion of the implementation of finite-difference methods as elements. Next we review the generalized SBP approach. In Section III we introduce a theoretical basis for SBP operators in multiple dimensions and provide examples on simplices in two and three dimensions.

II. One dimensional SBP operators

A. Classical SBP Operators

Our starting point is the classical SBP operator definition, proposed by Kreiss and Scherer [7] with the purpose of bringing to higher-order finite-difference methods a systematic means of proving stability. These operators are defined as

Definition 1 Classical summation-by-parts operators: *Consider the domain* $[x_{\mathrm{L}}, x_{\mathrm{R}}]$. *The matrix* D_x *is a degree* p *classical one-dimensional SBP approximation to the first derivative* $\frac{\partial}{\partial x}$ *on the nodes* $S = \{x_{\mathrm{L}} + (i-1)h\}_{i=1}^{n}$, *where* $h = \frac{x_{\mathrm{R}} - x_{\mathrm{L}}}{n-1}$, *if*

1. $\mathsf{D}_x \boldsymbol{x}^{a_x} = a_x \boldsymbol{x}^{a_x - 1}$, $\forall\ a_x \leq p$;
2. $\mathsf{D}_x = \mathsf{H}^{-1}\mathsf{S}_x = \mathsf{H}^{-1}\left(\mathsf{Q}_x + \frac{1}{2}\mathsf{E}_{\mathrm{c}}\right)$, *where* Q_x *is antisymmetric, and* $\mathsf{E}_{\mathrm{c}} = \mathrm{diag}(-1, 0, \ldots, 0, 1)$, *and;*
3. H *is symmetric positive definite.*

Property 1 ensures that the difference matrix D_x is exact for the restriction of polynomials x^{a_x} onto the grid. The system of equations that needs to be solved to satisfy this property can equivalently be derived using Taylor series expansions. The second property (2) ensures provable stability, while the last property ensures that classical SBP operators result in a consistent discrete representation of integration by parts.

To show how these operators are used to discretize PDEs, we consider the linear convection equation

$$\frac{\partial \mathcal{U}}{\partial t} = -\frac{\partial \mathcal{U}}{\partial x}, \quad x \in [0, 1], \tag{1}$$

with the following boundary condition, where the initial condition is immaterial for the current discussion,

$$\mathcal{U}(0, t) = \mathcal{G}(t). \tag{2}$$

Using the classical diagonal-norm SBP first-derivative operator of order two, which leads to solutions of global order three, to discretize the spatial derivative in (1) results in the following ODE:

$$\frac{\mathrm{d}\boldsymbol{u}_h}{\mathrm{d}t} = -\mathsf{D}_x \boldsymbol{u}_h, \tag{3}$$

where, for now, we ignore the imposition of interface conditions, and, for simplicity, we focus on diagonal norm matrices. For $p = 2$ and a nodal distribution with n nodes, the diagonal norm matrix H is given as

$$\mathsf{H} = \frac{1}{n-1}\,\mathrm{diag}\left[\ \tfrac{17}{48}\quad \tfrac{59}{48}\quad \tfrac{43}{48}\quad \tfrac{49}{48}\quad 1\quad \ldots\quad 1\quad \tfrac{49}{48}\quad \tfrac{43}{48}\ \tfrac{59}{48}\quad \tfrac{17}{48}\ \right], \tag{4}$$

and

$$\mathsf{Q}_x = \left[\begin{array}{cccc|cccc|cccc}
0 & \frac{59}{96} & -\frac{1}{12} & -\frac{1}{32} & & & & & & & & \\
-\frac{59}{96} & 0 & \frac{59}{96} & & & & & & & & & \\
\frac{1}{12} & -\frac{59}{96} & 0 & \frac{59}{96} & -\frac{1}{12} & & & & & & & \\
\frac{1}{32} & 0 & -\frac{59}{96} & 0 & \frac{2}{3} & -\frac{1}{12} & & & & & & \\
\hline
 & & \frac{1}{12} & -\frac{2}{3} & 0 & \frac{2}{3} & -\frac{1}{12} & & & & & \\
 & & & \ddots & \ddots & \ddots & \ddots & \ddots & & & & \\
 & & & & \frac{1}{12} & -\frac{2}{3} & 0 & \frac{2}{3} & -\frac{1}{12} & & & \\
\hline
 & & & & & \frac{1}{12} & -\frac{2}{3} & 0 & \frac{59}{96} & 0 & -\frac{1}{32} & \\
 & & & & & & \frac{1}{12} & -\frac{59}{96} & 0 & \frac{59}{96} & -\frac{1}{12} & \\
 & & & & & & & -\frac{59}{96} & 0 & \frac{59}{96} & & \\
 & & & & & & & \frac{1}{32} & \frac{1}{12} & -\frac{59}{96} & 0 &
\end{array}\right]. \tag{5}$$

The repeating interior operator is highlighted in blue, while the green triangles contain entries that originate from the repeating interior operator and ensure that the resultant Q_x is skew symmetric. The entries associated with the boundary operators are shown in the grey boxes. The matrix $\mathsf{D}_x = \mathsf{H}^{-1}\mathsf{S}_x$ is given as

$$\mathsf{D}_x = (n-1)\left[\begin{array}{cccccccccccc}
-\frac{24}{17} & \frac{59}{34} & -\frac{4}{17} & -\frac{3}{34} & & & & & & & & \\
-\frac{1}{2} & 0 & \frac{1}{2} & & & & & & & & & \\
\frac{4}{43} & -\frac{59}{86} & 0 & \frac{59}{86} & -\frac{4}{43} & & & & & & & \\
\frac{3}{98} & 0 & -\frac{59}{98} & 0 & \frac{32}{49} & -\frac{4}{49} & & & & & & \\
 & & \frac{1}{12} & -\frac{2}{3} & 0 & \frac{2}{3} & -\frac{1}{12} & & & & & \\
 & & & \ddots & \ddots & \ddots & \ddots & \ddots & & & & \\
 & & & & \frac{1}{12} & -\frac{2}{3} & 0 & \frac{2}{3} & -\frac{1}{12} & & & \\
 & & & & & \frac{4}{49} & -\frac{32}{49} & 0 & \frac{59}{98} & 0 & -\frac{3}{98} & \\
 & & & & & & \frac{4}{43} & -\frac{59}{86} & 0 & \frac{59}{86} & -\frac{4}{43} & \\
 & & & & & & & & -\frac{1}{2} & 0 & \frac{1}{2} & \\
 & & & & & & & \frac{3}{34} & \frac{4}{17} & -\frac{59}{34} & \frac{24}{17} &
\end{array}\right]. \tag{6}$$

To apply this operator on a nodal distribution with a larger number of nodes, the matrix is expanded by inserting additional interior operators, which does not require a change to the operators near the boundaries. The entries in Q_x and H are specified by satisfying the degree conditions (1) and the constraint that H be positive definite.

For diagonal-norm classical FD-SBP operators up to $p \leq 4$, using $2p$ boundary operators at the first and last $2p$ nodes leads to unique H that are positive definite. For $p > 4$ increasing numbers of boundary nodes need to be used in order to introduce degrees of freedom such that a positive-definite H can be found.

Boundary conditions can be weakly enforced using SATs. The discretization of the linear convection equation using a SAT to enforce the left boundary condition is given as

$$\frac{\mathrm{d}\boldsymbol{u}_h}{\mathrm{d}x} = -\mathsf{D}_x\boldsymbol{u}_h + \boldsymbol{SAT}_L = \mathsf{A}_h\boldsymbol{u}_h + \boldsymbol{b} \tag{7}$$

where the SAT is

$$\boldsymbol{SAT}_L = \sigma_L\left(u_1 - \mathcal{G}(t)\right)\mathsf{H}^{-1}\boldsymbol{e}_1, \tag{8}$$

$\boldsymbol{e}_1 = \begin{bmatrix} 1 & 0 & \dots & 0 \end{bmatrix}^{\mathrm{T}}$, and the range of σ_L is determined by conservation, accuracy, and stability. The term $\boldsymbol{SAT}_L$ in (7) enforces the boundary condition weakly; that is, at the boundary node, both the PDE and the boundary condition are enforced simultaneously.

Using $\sigma_L = -1$ results in a discretization that is conservative, stable, and dual-consistent [17], which leads to superconvergent approximations of functionals. Using this value of the penalty parameter, results in the following matrix operator A_h in (7):

$$\mathsf{A}_h = (n-1)\begin{bmatrix}
\boxed{-\frac{24}{17}} & -\frac{59}{34} & \frac{4}{17} & \frac{3}{34} & & & & & & & \\
\frac{1}{2} & 0 & -\frac{1}{2} & 0 & & & & & & & \\
-\frac{4}{43} & \frac{59}{86} & 0 & -\frac{59}{86} & \frac{4}{43} & & & & & & \\
-\frac{3}{98} & 0 & \frac{59}{98} & 0 & -\frac{32}{49} & \frac{4}{49} & & & & & \\
 & & -\frac{1}{12} & \frac{2}{3} & 0 & -\frac{2}{3} & \frac{1}{12} & & & & \\
 & & & \ddots & \ddots & \ddots & \ddots & \ddots & & & \\
 & & & & -\frac{1}{12} & \frac{2}{3} & 0 & -\frac{2}{3} & \frac{1}{12} & & \\
 & & & & & -\frac{4}{49} & \frac{32}{49} & 0 & -\frac{59}{98} & 0 & \frac{3}{98} \\
 & & & & & & -\frac{4}{43} & \frac{59}{86} & 0 & -\frac{59}{86} & \frac{4}{43} \\
 & & & & & & & 0 & \frac{1}{2} & 0 & -\frac{1}{2} \\
 & & & & & & & -\frac{3}{34} & -\frac{4}{17} & \frac{59}{34} & -\frac{24}{17}
\end{bmatrix}, \tag{9}$$

where the entry modified by the SAT has been highlighted in blue. We will use the value $\sigma_L = -1$ throughout this section.

B. Finite Difference Operators Implemented as Elements

Now consider a domain with 18 grid nodes divided into two blocks of nine nodes each. It is necessary to couple the solution in the first block, $\boldsymbol{u}_h$, to the solution in the second block $\boldsymbol{v}_h$. This can be accomplished using SATs. For the first element, the required coupling SAT is

$$\boldsymbol{SAT}_{\boldsymbol{u}_h} = \sigma_{\boldsymbol{u}_h}\,(u_n - v_1)\,\mathsf{H}^{-1}\boldsymbol{e}_n, \tag{10}$$

where $\boldsymbol{e}_n = \begin{bmatrix} 0 & \dots & 0 & 1 \end{bmatrix}^{\mathrm{T}}$, while for the second element, the SAT is given by

$$\boldsymbol{SAT}_{\boldsymbol{v}_h} = \sigma_{\boldsymbol{v}_h}\,(v_1 - u_n)\,\mathsf{H}^{-1}\boldsymbol{e}_1. \tag{11}$$

The choice $\sigma_{\boldsymbol{u}_h} = \frac{1}{2}$ and $\sigma_{\boldsymbol{v}_h} = -\frac{1}{2}$ results in a nondissipative interface coupling [18], and this is what we use for the remainder of this section. With this choice of SAT penalty parameters we get

$$\mathsf{A}_h = 4\begin{bmatrix}
\boxed{-\frac{24}{17}} & -\frac{59}{34} & \frac{4}{17} & \frac{3}{34} & & & & & & & & & & & & & & & & \\
\frac{1}{2} & 0 & -\frac{1}{2} & 0 & & & & & & & & & & & & & & & & \\
-\frac{4}{43} & \frac{59}{86} & 0 & -\frac{59}{86} & \frac{4}{43} & & & & & & & & & & & & & & & \\
-\frac{3}{98} & 0 & \frac{59}{98} & 0 & -\frac{32}{49} & \frac{4}{49} & & & & & & & & & & & & & & \\
 & & -\frac{1}{12} & \frac{2}{3} & 0 & -\frac{2}{3} & \frac{1}{12} & & & & & & & & & & & & & \\
 & & & -\frac{4}{49} & \frac{32}{49} & 0 & -\frac{59}{98} & 0 & \frac{3}{98} & & & & & & & & & & & \\
 & & & & -\frac{4}{43} & \frac{59}{86} & 0 & -\frac{59}{86} & \frac{4}{43} & & & & & & & & & & & \\
 & & & & & 0 & \frac{1}{2} & 0 & -\frac{1}{2} & & & & & & & & & & & \\
 & & & & & -\frac{3}{34} & -\frac{4}{17} & \frac{59}{34} & \boxed{0} & \boxed{-\frac{24}{17}} & & & & & & & & & & \\
 & & & & & & & & \boxed{\frac{24}{17}} & \boxed{0} & -\frac{59}{34} & \frac{4}{17} & \frac{3}{34} & & & & & & & \\
 & & & & & & & & & \frac{1}{2} & 0 & -\frac{1}{2} & 0 & & & & & & & \\
 & & & & & & & & & -\frac{4}{43} & \frac{59}{86} & 0 & -\frac{59}{86} & \frac{4}{43} & & & & & & \\
 & & & & & & & & & -\frac{3}{98} & 0 & \frac{59}{98} & 0 & -\frac{32}{49} & \frac{4}{49} & & & & & \\
 & & & & & & & & & & & -\frac{1}{12} & \frac{2}{3} & 0 & -\frac{2}{3} & \frac{1}{12} & & & & \\
 & & & & & & & & & & & & -\frac{4}{49} & \frac{32}{49} & 0 & -\frac{59}{98} & 0 & \frac{3}{98} & & \\
 & & & & & & & & & & & & & -\frac{4}{43} & \frac{59}{86} & 0 & -\frac{59}{86} & \frac{4}{43} & & \\
 & & & & & & & & & & & & & & 0 & \frac{1}{2} & 0 & -\frac{1}{2} & & \\
 & & & & & & & & & & & & & & -\frac{3}{34} & -\frac{4}{17} & \frac{59}{34} & \boxed{-\frac{24}{17}} &
\end{bmatrix}. \tag{12}$$

The highlighted entries are those that have been modified by the SATs. In the traditional finite-difference approach, mesh refinement is accomplished by increasing the number of nodes where the interior operator is applied, as follows:

$$\mathsf{A}_h = \frac{n-1}{2}\begin{bmatrix}
-\frac{24}{17} & -\frac{59}{34} & \frac{4}{17} & \frac{3}{34} & & & & & & & & & & & & & & & & \\
\frac{1}{2} & 0 & -\frac{1}{2} & 0 & & & & & & & & & & & & & & & & \\
-\frac{4}{43} & \frac{59}{86} & 0 & -\frac{59}{86} & \frac{4}{43} & & & & & & & & & & & & & & & \\
-\frac{3}{98} & 0 & \frac{59}{98} & 0 & -\frac{32}{49} & \frac{4}{49} & & & & & & & & & & & & & & \\
 & & -\frac{1}{12} & \frac{2}{3} & 0 & -\frac{2}{3} & \frac{1}{12} & & & & & & & & & & & & & \\
 & & & \ddots & \ddots & \ddots & \ddots & \ddots & & & & & & & & & & & & \\
 & & & & -\frac{1}{12} & \frac{2}{3} & 0 & -\frac{2}{3} & \frac{1}{12} & & & & & & & & & & & \\
 & & & & & -\frac{4}{49} & \frac{32}{49} & 0 & -\frac{59}{98} & 0 & \frac{3}{98} & & & & & & & & & \\
 & & & & & & -\frac{4}{43} & \frac{59}{86} & 0 & -\frac{59}{86} & \frac{4}{43} & & & & & & & & & \\
 & & & & & & & 0 & \frac{1}{2} & 0 & -\frac{1}{2} & & & & & & & & & \\
 & & & & & & & -\frac{3}{34} & -\frac{4}{17} & \frac{59}{34} & 0 & -\frac{24}{17} & & & & & & & & \\
 & & & & & & & & & & \frac{24}{17} & 0 & -\frac{59}{34} & \frac{4}{17} & \frac{3}{34} & & & & & \\
 & & & & & & & & & & & \frac{1}{2} & 0 & -\frac{1}{2} & 0 & & & & & \\
 & & & & & & & & & & & -\frac{4}{43} & \frac{59}{86} & 0 & -\frac{59}{86} & \frac{4}{43} & & & & \\
 & & & & & & & & & & & -\frac{3}{98} & 0 & \frac{59}{98} & 0 & -\frac{32}{49} & \frac{4}{49} & & & \\
 & & & & & & & & & & & & & -\frac{1}{12} & \frac{2}{3} & 0 & -\frac{2}{3} & \frac{1}{12} & & \\
 & & & & & & & & & & & & & & \ddots & \ddots & \ddots & \ddots & \ddots & \\
 & & & & & & & & & & & & & & & -\frac{1}{12} & \frac{2}{3} & 0 & -\frac{2}{3} & \frac{1}{12} \\
 & & & & & & & & & & & & & & & & -\frac{4}{49} & \frac{32}{49} & 0 & -\frac{59}{98} & 0 & \frac{3}{98} \\
 & & & & & & & & & & & & & & & & & -\frac{4}{43} & \frac{59}{86} & 0 & -\frac{59}{86} & \frac{4}{43} \\
 & & & & & & & & & & & & & & & & & & 0 & \frac{1}{2} & 0 & -\frac{1}{2} \\
 & & & & & & & & & & & & & & & & & & -\frac{3}{34} & -\frac{4}{17} & \frac{59}{34} & -\frac{24}{17}
\end{bmatrix}. \tag{13}$$

However, one can alternatively keep the block size at nine and increase the number of blocks, leading to

the following matrix operator with N elements:

$$\mathsf{A}_h = \begin{bmatrix} \hat{\mathsf{A}}_h & \mathsf{SAT}_{\boldsymbol{u}_h} & & & & \\ \mathsf{SAT}_{\boldsymbol{v}_h} & \tilde{\mathsf{A}}_h & \mathsf{SAT}_{\boldsymbol{u}_h} & & & \\ & \ddots & \ddots & \cdots & & \\ & & \mathsf{SAT}_{\boldsymbol{v}_h} & \tilde{\mathsf{A}}_h & \mathsf{SAT}_{\boldsymbol{u}_h} & \\ & & & \mathsf{SAT}_{\boldsymbol{v}_h} & \breve{\mathsf{A}}_h \end{bmatrix}, \tag{14}$$

where

$$\hat{\mathsf{A}}_h = \frac{8}{N}\begin{bmatrix} -\frac{24}{17} & -\frac{59}{34} & \frac{4}{17} & \frac{3}{34} & & & & & \\ \frac{1}{2} & 0 & -\frac{1}{2} & 0 & & & & & \\ -\frac{4}{43} & \frac{59}{86} & 0 & -\frac{59}{86} & \frac{4}{43} & & & & \\ -\frac{3}{98} & 0 & \frac{59}{98} & 0 & -\frac{32}{49} & \frac{4}{49} & & & \\ & & -\frac{1}{12} & \frac{2}{3} & 0 & -\frac{2}{3} & \frac{1}{12} & & \\ & & & -\frac{4}{49} & \frac{32}{49} & 0 & -\frac{59}{98} & 0 & \frac{3}{98} \\ & & & & -\frac{4}{43} & \frac{59}{86} & 0 & -\frac{59}{86} & \frac{4}{43} \\ & & & & & 0 & \frac{1}{2} & 0 & -\frac{1}{2} \\ & & & & & -\frac{3}{34} & -\frac{4}{17} & \frac{59}{34} & 0 \end{bmatrix}, \tilde{\mathsf{A}}_h = \frac{8}{N}\begin{bmatrix} 0 & -\frac{59}{34} & \frac{4}{17} & \frac{3}{34} & & & & & \\ \frac{1}{2} & 0 & -\frac{1}{2} & 0 & & & & & \\ -\frac{4}{43} & \frac{59}{86} & 0 & -\frac{59}{86} & \frac{4}{43} & & & & \\ -\frac{3}{98} & 0 & \frac{59}{98} & 0 & -\frac{32}{49} & \frac{4}{49} & & & \\ & & -\frac{1}{12} & \frac{2}{3} & 0 & -\frac{2}{3} & \frac{1}{12} & & \\ & & & -\frac{4}{49} & \frac{32}{49} & 0 & -\frac{59}{98} & 0 & \frac{3}{98} \\ & & & & -\frac{4}{43} & \frac{59}{86} & 0 & -\frac{59}{86} & \frac{4}{43} \\ & & & & & 0 & \frac{1}{2} & 0 & -\frac{1}{2} \\ & & & & & -\frac{3}{34} & -\frac{4}{17} & \frac{59}{34} & 0 \end{bmatrix},$$

$$\breve{\mathsf{A}}_h = \frac{8}{N}\begin{bmatrix} 0 & -\frac{59}{34} & \frac{4}{17} & \frac{3}{34} & & & & & \\ \frac{1}{2} & 0 & -\frac{1}{2} & 0 & & & & & \\ -\frac{4}{43} & \frac{59}{86} & 0 & -\frac{59}{86} & \frac{4}{43} & & & & \\ -\frac{3}{98} & 0 & \frac{59}{98} & 0 & -\frac{32}{49} & \frac{4}{49} & & & \\ & & -\frac{1}{12} & \frac{2}{3} & 0 & -\frac{2}{3} & \frac{1}{12} & & \\ & & & -\frac{4}{49} & \frac{32}{49} & 0 & -\frac{59}{98} & 0 & \frac{3}{98} \\ & & & & -\frac{4}{43} & \frac{59}{86} & 0 & -\frac{59}{86} & \frac{4}{43} \\ & & & & & 0 & \frac{1}{2} & 0 & -\frac{1}{2} \\ & & & & & -\frac{3}{34} & -\frac{4}{17} & \frac{59}{34} & -\frac{24}{17} \end{bmatrix}, \tag{15}$$

$\mathsf{SAT}_{\boldsymbol{v}_h}$ is a 9×9 matrix given by

$$\mathsf{SAT}_{\boldsymbol{v}_h} = \frac{8}{N}\begin{bmatrix} 0 & \dots & 0 & \frac{24}{17} \\ 0 & \dots & 0 & 0 \\ \vdots & & \vdots & \vdots \\ 0 & \dots & 0 & 0 \end{bmatrix}, \tag{16}$$

and $\mathsf{SAT}_{\boldsymbol{u}_h}$ is a 9×9 matrix given by

$$\mathsf{SAT}_{\boldsymbol{u}_h} = \frac{8}{N}\begin{bmatrix} 0 & 0 & \dots & 0 \\ \vdots & \vdots & & \vdots \\ 0 & 0 & \dots & 0 \\ -\frac{24}{17} & 0 & \dots & 0 \end{bmatrix}. \tag{17}$$

This describes the element approach, and the 9×9 blocks can be considered to be elements, even though their origin is as finite-difference operators. These elements can be arbitrarily large, but they have a minimum size. For this case, with $p = 2$, the minimum size is nine nodes such that at least one matrix row corresponds to the interior operator.

C. Generalized SBP Operators

In the last section, we have shown that classical SBP operators can be applied using either the traditional finite-difference approach or the element approach. As described in the Introduction, the SBP concept can

be applied to a much broader set of operators. The generalized SBP definition is given by the following [16]:

Definition 2 Generalized summation-by-parts operators: *Consider the domain* $[x_{\mathrm{L}}, x_{\mathrm{R}}]$ *and the set of nodes* $S = \{x_i\}_{i=1}^{n}$*, which is not necessarily uniform and may not include nodes at the boundaries. The matrix* D_x *is a degree* p *one-dimensional generalized SBP approximation to the first derivative* $\frac{\partial}{\partial x}$ *if*

1. $\mathsf{D}_x \boldsymbol{x}^{a_x} = a_x \boldsymbol{x}^{a_x - 1}$, $\forall\, a_x \leq p$;
2. $\mathsf{D}_x = \mathsf{H}^{-1}\mathsf{S}_x = \mathsf{H}^{-1}\left(\mathsf{Q}_x + \frac{1}{2}\mathsf{E}_x\right)$, *where* Q_x *is antisymmetric;*
3. $\left(\boldsymbol{x}^i\right)^{\mathrm{T}} \mathsf{E}_x \boldsymbol{x}^j = x_{\mathrm{R}}^{i+j} - x_{\mathrm{L}}^{i+j}$, $\forall\, i + j \leq r$, *where* $r \geq p$, E_x *is symmetric, and;*
4. H *is symmetric positive definite.*

An important difference from Definition 1 is the change from E_{c} to E_x; this frees us from having to include boundary nodes in the nodal distribution, while retaining the ability to prove stability in exactly the same way as is done for classical SBP operators. The definition of E_x is motivated by approximating the term $\mathcal{V}\mathcal{U}\big|_{x_{\mathrm{L}}}^{x_{\mathrm{R}}}$ that results from integration by parts in one dimension. As we shall see in Section III, this idea motivates the definition of multidimensional SBP operators for unstructured meshes.

As an example, consider a $p = 2$ generalized SBP operator constructed on the hybrid Gauss-trapezoidal-Lobatto quadrature nodes proposed by Alpert [19]. On nine nodes, which is the minimum number of nodes for this operator, the difference matrix is given as

$$\mathsf{D}_x = 8 \begin{bmatrix} -\frac{864}{553} & \frac{408811}{209034} & -\frac{2901}{7742} & -\frac{278}{14931} & & & & & \\ -\frac{41}{78} & 0 & \frac{15}{26} & -\frac{2}{39} & & & & & \\ \frac{967}{7932} & -\frac{49855}{71388} & 0 & \frac{11800}{17847} & -\frac{56}{661} & & & & \\ \frac{139}{23460} & \frac{9971}{164220} & -\frac{1770}{2737} & 0 & \frac{1296}{1955} & -\frac{162}{1955} & & & \\ & & \frac{1}{12} & -\frac{2}{3} & 0 & \frac{2}{3} & -\frac{1}{12} & & \\ & & & \frac{162}{1955} & -\frac{1296}{1955} & 0 & \frac{1770}{2737} & -\frac{9971}{164220} & -\frac{139}{23460} \\ & & & & \frac{56}{661} & -\frac{11800}{17847} & 0 & \frac{49855}{71388} & -\frac{967}{7932} \\ & & & & & \frac{2}{39} & -\frac{15}{26} & 0 & \frac{41}{78} \\ & & & & & \frac{278}{14931} & \frac{2901}{7742} & -\frac{408811}{209034} & \frac{864}{553} \end{bmatrix}, \tag{18}$$

the diagonal-norm matrix is given by

$$\mathsf{H} = \frac{1}{8}\,\mathrm{diag}\left[\begin{array}{ccccccccc} \frac{553}{1728} & \frac{129623}{108864} & \frac{661}{672} & \frac{1955}{1944} & 1 & \frac{1955}{1944} & \frac{661}{672} & \frac{129623}{108864} & \frac{553}{1728} \end{array}\right], \tag{19}$$

and the nodal distribution is given by

$$\boldsymbol{x} = \frac{1}{8}\left[\begin{array}{ccccccccc} 0 & \frac{12}{13} & 2 & 3 & 4 & 5 & 6 & (8 - \frac{12}{13}) & 8 \end{array}\right]^{\mathrm{T}}. \tag{20}$$

Using two nine-node elements with the same SAT coefficients as in the previous section results in

$$\mathsf{A}_h = 4\left[\begin{array}{ccccccccccccccccccc}
-\frac{864}{553} & -\frac{408811}{209034} & \frac{2901}{7742} & \frac{278}{14931} & & & & & & & & & & & & & & & \\
\frac{41}{78} & 0 & -\frac{15}{26} & \frac{2}{39} & & & & & & & & & & & & & & & \\
-\frac{967}{7932} & \frac{49855}{71388} & 0 & -\frac{11800}{17847} & \frac{56}{661} & & & & & & & & & & & & & & \\
-\frac{139}{23460} & -\frac{9971}{164220} & \frac{1770}{2737} & 0 & -\frac{1296}{1955} & \frac{162}{1955} & & & & & & & & & & & & & \\
 & & -\frac{1}{12} & \frac{2}{3} & 0 & -\frac{2}{3} & \frac{1}{12} & & & & & & & & & & & & \\
 & & & -\frac{162}{1955} & \frac{1296}{1955} & 0 & -\frac{1770}{2737} & \frac{9971}{164220} & \frac{139}{23460} & & & & & & & & & & \\
 & & & & -\frac{56}{661} & \frac{11800}{17847} & 0 & -\frac{49855}{71388} & \frac{967}{7932} & & & & & & & & & & \\
 & & & & & -\frac{2}{39} & \frac{15}{26} & 0 & -\frac{41}{78} & & & & & & & & & & \\
 & & & & & -\frac{278}{14931} & -\frac{2901}{7742} & \frac{408811}{209034} & 0 & -\frac{864}{553} & -\frac{408811}{209034} & \frac{2901}{7742} & \frac{278}{14931} & & & & & & \\
 & & & & & & & & \frac{864}{553} & 0 & 0 & -\frac{15}{26} & \frac{2}{39} & & & & & & \\
 & & & & & & & & & \frac{41}{78} & 0 & 0 & -\frac{11800}{17847} & \frac{56}{661} & & & & & \\
 & & & & & & & & & -\frac{967}{7932} & \frac{49855}{71388} & \frac{1770}{2737} & 0 & -\frac{1296}{1955} & \frac{162}{1955} & & & & \\
 & & & & & & & & & -\frac{139}{23460} & -\frac{9971}{164220} & -\frac{1}{12} & \frac{2}{3} & 0 & -\frac{2}{3} & \frac{1}{12} & & & \\
 & & & & & & & & & & & & -\frac{162}{1955} & \frac{1296}{1955} & 0 & -\frac{1770}{2737} & \frac{9971}{164220} & \frac{139}{23460} & \\
 & & & & & & & & & & & & & -\frac{56}{661} & \frac{11800}{17847} & 0 & -\frac{49855}{71388} & \frac{967}{7932} & \\
 & & & & & & & & & & & & & & -\frac{2}{39} & \frac{15}{26} & 0 & -\frac{41}{78} & \\
 & & & & & & & & & & & & & & -\frac{278}{14931} & -\frac{2901}{7742} & \frac{408811}{209034} & -\frac{864}{553} &
\end{array}\right]. \tag{21}$$

This is an example of a GSBP operator that can be implemented either in the traditional finite-difference manner by increasing the number of matrix rows where the interior operator is applied or in the element manner in which the element size is fixed and the number of elements is increased. However, in contrast to classical operators, the nodal distribution has a number of nodes that are not evenly spaced, in this case one node at either boundary. The benefit of this is that truncation error terms from the boundary terms can be significantly reduced. This results in solutions that have a smaller global error compared to classical SBP operators and therefore leads to more efficient discretization methods [20, 21]. Similar operators have been derived by Mattsson *et al.* [22].

Next we consider a GSBP operator of fixed size that can therefore only be implemented as an element. We construct a diagonal-norm GSBP operator on the Chebyshev-Gauss-Lobatto quadrature nodes [16], which have the following nodal distribution for five nodes:

$$\boldsymbol{x} = \frac{1}{2}\begin{bmatrix} -1 & -\frac{1}{2}\sqrt{2} & 0 & \frac{1}{2}\sqrt{2} & 1 \end{bmatrix}^{\mathrm{T}} + \left(\frac{1}{2}\right)\mathbf{1}, \tag{22}$$

where $\mathbf{1}$ is a vector of ones. The operator is given by

$$\mathsf{D}_x = 2\begin{bmatrix}
-\frac{15}{2} & 8+2\sqrt{2} & -6 & 8-2\sqrt{2} & -\frac{5}{2} \\
-1-\frac{1}{4}\sqrt{2} & 0 & \frac{3}{2}\sqrt{2} & -\sqrt{2} & 1-\frac{1}{4}\sqrt{2} \\
\frac{1}{2} & -\sqrt{2} & 0 & \sqrt{2} & -\frac{1}{2} \\
-1+\frac{1}{4}\sqrt{2} & \sqrt{2} & -\frac{3}{2}\sqrt{2} & 0 & 1+\frac{1}{4}\sqrt{2} \\
\frac{5}{2} & -8+2\sqrt{2} & 6 & -8-2\sqrt{2} & \frac{15}{2}
\end{bmatrix}, \tag{23}$$

the norm matrix is

$$\mathsf{H} = \frac{1}{2}\,\mathrm{diag}\begin{bmatrix} \frac{1}{15} & \frac{8}{15} & \frac{4}{5} & \frac{8}{15} & \frac{1}{15} \end{bmatrix}. \tag{24}$$

Using two elements again with the same SAT coefficients results in

$$\mathsf{A}_h = 2\begin{bmatrix}
-\frac{15}{2} & -8-2\sqrt{2} & 6 & -8+2\sqrt{2} & \frac{5}{2} & & & & & \\
1+\frac{1}{4}\sqrt{2} & 0 & -\frac{3}{2}\sqrt{2} & \sqrt{2} & -1+\frac{1}{4}\sqrt{2} & & & & & \\
-\frac{1}{2} & \sqrt{2} & 0 & -\sqrt{2} & \frac{1}{2} & & & & & \\
1-\frac{1}{4}\sqrt{2} & -\sqrt{2} & \frac{3}{2}\sqrt{2} & 0 & -1-\frac{1}{4}\sqrt{2} & & & & & \\
-\frac{5}{2} & 8-2\sqrt{2} & -6 & 8+2\sqrt{2} & 0 & -\frac{15}{2} & & & & \\
 & & & & \frac{15}{2} & 0 & -8-2\sqrt{2} & 6 & -8+2\sqrt{2} & \frac{5}{2} \\
 & & & & & 1+\frac{1}{4}\sqrt{2} & 0 & -\frac{3}{2}\sqrt{2} & \sqrt{2} & -1+\frac{1}{4}\sqrt{2} \\
 & & & & & -\frac{1}{2} & \sqrt{2} & 0 & -\sqrt{2} & \frac{1}{2} \\
 & & & & & 1-\frac{1}{4}\sqrt{2} & -\sqrt{2} & \frac{3}{2}\sqrt{2} & 0 & -1-\frac{1}{4}\sqrt{2} \\
 & & & & & -\frac{5}{2} & 8-2\sqrt{2} & -6 & 8+2\sqrt{2} & -\frac{15}{2}
\end{bmatrix}. \tag{25}$$

The various operators shown above demonstrate some of the operators that can be constructed with the SBP property. With the SATs shown, these schemes are provably stable, but they can be used with other methods for coupling the elements as well. In the context of the linear convection equation on a uniform mesh, the traditional finite-difference approach with a repeating interior operator is generally the most accurate approach. The boundary operators are typically less accurate than the interior operator; with the traditional approach their effect is minimized. However, as discussed in the introduction, the element approach offers opportunities for h and p refinement and extends to unstructured grids in multiple dimensions. This suggests that a hybrid approach that combines the traditional finite-difference approach with an element approach could be efficient. Together with the extensions afforded by the generalized SBP definition, the perspective discussed here in which SBP operators are applied as elements paves the way for multidimensional SBP operators. This enables the provable stability of the SBP approach to be brought to methods for unstructured grids, with the advantages described in the Introduction. As noted previously, some finite-element methods have the SBP property, and these methods can be applied on unstructured grids. However, the current approach enables the development of very general methods in multiple dimensions with the SBP property and thus provable stability. This generality arises as a result of the fact that, in contrast to finite-element methods, SBP operators do not require the existence of a basis in closed form. This is explored in the next section.

III. Multidimensional SBP Operators for Unstructured Grids

A. Formal Definition

Our proposed definition for multidimensional SBP operators is given below. The definition extends the notion of generalized one-dimensional SBP operators proposed in Ref. [16] and is inspired by the classical SBP operators of Kreiss and Scherer [7]. In the definition, the vectors $\boldsymbol{x}^{a_x}$ and $\boldsymbol{y}^{a_y}$ are the monomials x^{a_x} and y^{a_y} evaluated at the nodes, and $\circ$ denotes the Hadamard product.

Definition 3 Two-dimensional summation-by-parts operators: *Consider an open and bounded domain $\Omega \subset \mathbb{R}^2$ with a piecewise-smooth boundary Γ. The matrix D_x is a degree p SBP approximation to the first derivative $\frac{\partial}{\partial x}$ on the nodes $S = \{(x_i, y_i)\}_{i=1}^n$ if*

1. $\mathsf{D}_x \boldsymbol{x}^{a_x} \circ \boldsymbol{y}^{a_y} = a_x \boldsymbol{x}^{a_x - 1} \circ \boldsymbol{y}^{a_y}$, $\forall\, a_x + a_y \leq p$;
2. $\mathsf{D}_x = \mathsf{H}^{-1}\mathsf{S}_x = \mathsf{H}^{-1}\left(\mathsf{Q}_x + \frac{1}{2}\mathsf{E}_x\right)$, *where Q_x is antisymmetric, and E_x is symmetric;*
3. H *is symmetric positive definite, and;*
4. $\left(\boldsymbol{x}^{a_x} \circ \boldsymbol{y}^{a_y}\right)^{\mathrm{T}} \mathsf{E}_x \boldsymbol{x}^{b_x} \circ \boldsymbol{y}^{b_y} = \oint_\Gamma x^{a_x + b_x} y^{a_y + b_y} n_x \mathrm{d}\Gamma, \qquad \forall\, a_x + a_y, b_x + b_y \leq \tau_{\mathsf{E}_x}$,

   where $\tau_{\mathsf{E}_x} \geq p$ and $\boldsymbol{n} = [n_x, n_y]^{\mathrm{T}}$ is the outward pointing unit normal to the surface Γ.

As with the one-dimensional operator definitions, each of the properties in Definition 3 plays an important role. Property 1 ensures accuracy by requiring that the SBP operators are exact for polynomials of total

degree p. Property 2 is needed in order to mimic integration by parts, which is vital for proving time stability. Property 3 guarantees that the matrix H can be used to define a norm, which is also needed to prove stability.

Properties 1, 2, and 3 are also present in the definitions of classical SBP operators. The last property, Property 4, is introduced in the multidimensional case to ensure that E_x not only mimics the surface integral in the integration-by-parts formula, but approximates it to some order. A similar property is required by generalized one-dimensional SBP operators; see Definition 2.

B. Multidimensional SBP Operators with Diagonal Norms

In this section we consider the implications of Definition 3 when the matrix H is diagonal. Perhaps the most important implication is the following existence theorem.

Theorem 1 *Let $n_{\min} = (p+1)(p+2)/2$ be the dimension of the polynomial basis of degree p in two dimensions, and consider the node set $S = \{(x_i, y_i)\}_{i=1}^{n}$ with $n \geq n_{\min}$ nodes. Define the generalized Vandermonde matrix $\mathsf{V} \in \mathbb{R}^{n \times n_{\min}}$ whose columns are the monomial-basis elements evaluated at the nodes;*

$$\mathsf{V}_{:,k} = \boldsymbol{x}^i \circ \boldsymbol{y}^{j-i}, \qquad k = \frac{j(j+1)}{2} + i + 1, \quad \forall\, j = 0, 1, \ldots, p, \quad i = 0, 1, \ldots, j.$$

If the columns of V are linearly independent, then the existence of a cubature rule of degree $\tau_{\mathsf{H}} \geq 2p-1$ with positive weights is necessary and sufficient for the existence of degree p diagonal-norm SBP operators approximating the first derivatives $\frac{\partial}{\partial x}$ and $\frac{\partial}{\partial y}$ on the node set S.

See [23] for the proof. Theorem 1 tells us that the entries of H and nodes of an diagonal norm SBP operator define a cubature rule. This is consistent, by design, with classical [24] and generalized SBP theory [16]. Note that a similar theorem holds for higher dimensional SBP operators.

Theorem 1 also suggests a strategy for constructing SBP operators on a particular domain: first find a cubature rule with positive weights. This is the approach we take in Section III D when building SBP operators for simplices. Finally, we note that, while Theorem 1 provides conditions for existence, it does not say anything about the uniqueness of SBP operators of a particular degree on a given domain.

The connection between H and cubature opens the door to a number of other results that allow us to characterize S_x and its anti-symmetric part Q_x.

Theorem 2 *The matrix S_x of a degree p diagonal-norm multidimensional SBP operator defines a degree $\tau_{\mathsf{S}_x} = \min(\tau_{\mathsf{E}_x}, 2p)$ approximation to the bilinear form*

$$B_{\mathsf{S}_x}(\mathcal{V}, \mathcal{U}) = \int_\Omega \mathcal{V} \frac{\partial \mathcal{U}}{\partial x} \mathrm{d}\Omega. \tag{26}$$

Similarly, the matrix Q_x is a degree $\tau_{\mathsf{Q}_x} = \min(\tau_{\mathsf{E}_x}, 2p)$ approximation to the bilinear form

$$B_{\mathsf{Q}_x}(\mathcal{V}, \mathcal{U}) = \int_\Omega \mathcal{V} \frac{\partial \mathcal{U}}{\partial x} \mathrm{d}\Omega - \frac{1}{2} \oint_\Gamma \mathcal{V}\mathcal{U} n_x \mathrm{d}\Gamma. \tag{27}$$

Again, we refer the interested reader to Ref. [23] for the proof.

Suppose $\{\phi_i\}_{i=1}^{n}$ is a nodal basis, such that $\phi_i(x_j, y_j) = \delta_{ij}$. Then Theorem 2 provides an integral interpretation for the entries of S_x and Q_x:

$$(\mathsf{S}_x)_{i,j} = \int_\Omega \phi_i \frac{\partial \phi_j}{\partial x} \mathrm{d}\Omega, \qquad \text{and} \qquad (\mathsf{Q}_x)_{i,j} = \int_\Omega \phi_i \frac{\partial \phi_j}{\partial x} \mathrm{d}\Omega - \frac{1}{2} \oint_\Gamma \phi_i \phi_j n_x \mathrm{d}\Gamma.$$

Consequently, SBP discretizations have a finite-element-like variational interpretation; however, as mentioned earlier, the basis $\{\phi_i\}_{i=1}^{n}$ does not exist in closed form, in general. This is perhaps the key feature that distinguishes SBP operators from FEM ones.

C. Assembly of Global SBP Operators from Elemental Operators

The multidimensional SBP definition could, in theory, be applied directly to arbitrary domains. Indeed, such an approach was pursued by Chiu *et al.* [25, 26]. Their mesh-free operators are closely related to our proposed multidimensional SBP operators; the difference is that they do not include Property 4. A practical disadvantage of seeking SBP operators on a global domain *with prescribed node locations and stencils* is that a positive diagonal mass matrix may not exist for the desired accuracy [27]. This is not surprising in light of Theorem 1, since existence of the SBP operator is linked to the existence of a cubature with positive weights.

Instead of constructing SBP operators globally, we pursue a more conventional element-based approach; that is, construct SBP operators for individual elements or cells and then couple them. Even here there are multiple possibilities. The popular approach for tensor-product SBP operators on multiblock grids is to use simultaneous approximation terms to couple the elements. This is analogous to the discontinuous Galerkin method, including the multivalued nature of the solution along element interfaces.

Given the similarities between the DG finite-element method and the SBP-SAT method, one may ask if there would be a way to relate SBP discretizations to the continuous Galerkin finite-element method. In other words, can we use SBP operators defined on individual elements to assemble a single SBP operator on the global domain? The answer, provided formally in the following theorem, is yes.

Theorem 3 *Suppose the domain Ω is partitioned into a set of K non-overlapping subdomains $\Omega^{(k)}$ with boundaries $\Gamma^{(k)}$, and each subdomain is associated with a set of nodes $S^{(k)} \equiv \{(x_i^{(k)}, y_j^{(k)})\}_{i=1}^n$, such that $(x_i^{(k)}, y_i^{(k)}) \in \bar{\Omega}^{(k)}$. Let $\mathsf{D}_x^{(k)} = \left(\mathsf{H}^{(k)}\right)^{-1} \mathsf{S}_x^{(k)}$ be a degree p SBP operator for the first derivative $\partial/\partial x$ on the node set $S^{(k)}, k = 1, 2, \ldots, K$, and define*

$$\mathsf{H} \equiv \sum_{k=1}^{K} \sum_{i=1}^{n} \mathsf{H}_{i,i}^{(k)} \mathsf{Z}^{(k)}(i,i), \qquad \text{and} \qquad \mathsf{S}_x \equiv \sum_{k=1}^{K} \sum_{i=1}^{n} \sum_{j=1}^{n} \left(\mathsf{S}_x^{(k)}\right)_{i,j} \mathsf{Z}^{(k)}(i,j),$$

where the matrix $\mathsf{Z}^{(k)}(i,j)$ maps the local indices (i,j) on element k to global indices. Then $\mathsf{D}_x = \mathsf{H}^{-1}\mathsf{S}_x$ is a degree p SBP operator on the global node set $S \equiv \cup_k S^{(k)}$.

The proof, although somewhat tedious, is straightforward and can be found in Ref. [23].

Theorem 3 is significant, because it provides a systematic way to construct a *high-order finite-difference operator that satisfies the summation-by-parts definition on an arbitrary domain.* To the best of our knowledge, such a systematic construction has not been proposed or exploited in the SBP literature previously. Below, we use Theorem 3 to construct SBP operators on unstructured triangular grids.

D. SBP Operators for the Triangle and Tetrahedron

In this section, we describe the construction of multidimensional SBP operators for the triangle and tetrahedron. Unlike classical one-dimensional SBP operators, we do not restrict the operators to uniform node distributions, because Theorem 1 would then dictate that the entries of H be cubature weights on a uniform node distribution.

Our procedure for constructing SBP operators of degree p on simplex elements proceeds as follows.

1. Identify a cubature rule with positive weights that is exact for polynomials of degree $2p-1$ on the reference triangle or tetrahedron; we also require that $\binom{p+d-1}{d-1}$ nodes lie on each face of the elements, where d is the spatial dimension. For most of the operators considered in this work, cubature rules meeting our requirements can be found in the literature; see, for example, [28–31]. The one exception is the seventh degree cubature on the tetrahedron, which was constructed using methods from the literature [31–33]. The cubature weights are inserted into H and the cubature nodes become the nodes of the SBP operator.

2. Next, the boundary operators E_x, E_y, and E_z are constructed. Since the faces have $\binom{p+d-1}{d-1}$ nodes, we use a nodal polynomial basis to construct mass matrices for each face; see [34, pg. 187] for the details.

3. Finally, the antisymmetric matrices Q_x, Q_y, and Q_z are determined using the accuracy conditions. The accuracy conditions lead to systems with more equations then unknowns; however, the SBP definition ensures that these systems are consistent. In fact, for degrees $p \geq 3$ there are fewer constraints than

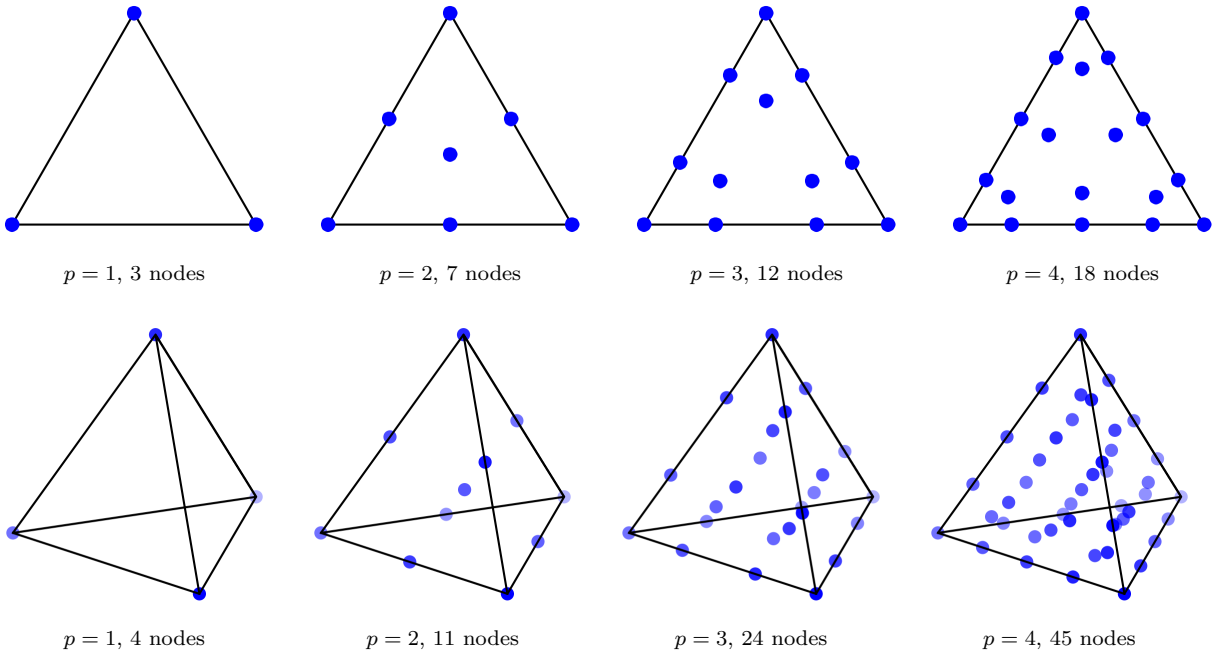

Figure 1. Node distributions for the SBP operators on triangles (upper figures) and tetrahedra (lower figures).

unknowns, so an infinite number of SBP operators exist; in this situation we take the minimum-norm solution to the least-squares problem [35].

We remark that each step in the above procedure is not unique: there are many different cubature rules that can be chosen, many different boundary operators that can be constructed, and many different ways the accuracy conditions can be satisfied, in general.

Figure 1 shows the nodal distributions of the simplex-based SBP operators considered in this work. The SBP operators themselves were generated using the Julia package SummationByParts, which is available for download on `github`[b].

The simplex SBP operators that result from the above procedure are similar to operators in the diagonal mass-matrix spectral-element (SE) method [29–31] and the spectral-difference (SD) method [36]. There are, however, some notable differences.

While the SBP matrix H is identical to the mass matrix used in the diagonal mass-matrix SE method, the stiffness matrices of the two methods differ. For example, in the SE method of Giraldo and Taylor [31], the stiffness matrix is defined using a polynomial basis with bubble functions, thus the integrand in the bilinear form is of higher degree than the cubature rule can integrate exactly. Consequently, the SE stiffness matrix does not have the symmetry structure of an SBP operator nor its stability properties.

The simplex SBP operators may also be regarded as SD operators in which the unknowns and fluxes are collocated. This collocation is typically avoided in the SD method, because the same formal accuracy can be achieved using fewer unknowns if the two sets of points are distinct [36]; however, the goal of reducing the number of unknowns on a per element basis assumes a discontinuous solution space. The perspective changes when elemental SBP operators are assembled into global operators, since some nodes will be shared by multiple elements.

[b] https://github.com/OptimalDesignLab/SummationByParts.jl

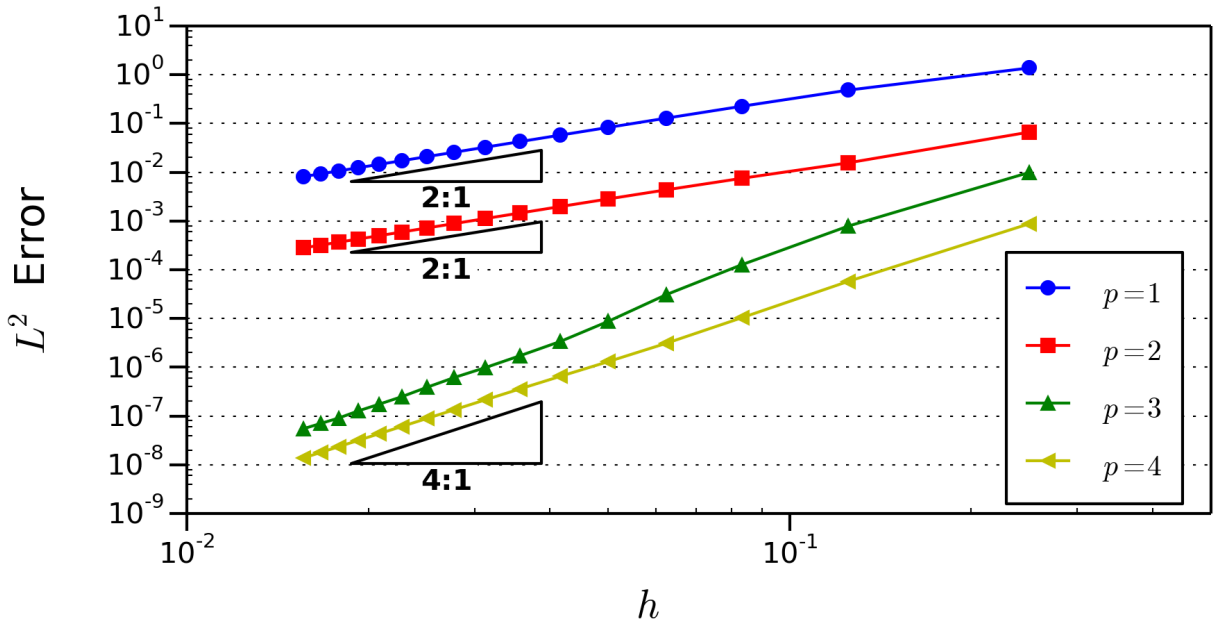

Figure 2. L^2 error between the solution at $t = 1$ and initial condition for different mesh spacing and operators.

E. Multidimensional SBP Results

The accuracy and stability properties of the triangular SBP operators are demonstrated by discretizing the two-dimensional linear convection equation on a periodic domain:

$$\frac{\partial \psi}{\partial t} + \boldsymbol{u} \cdot \nabla \psi = 0, \qquad \forall\ (x, y) \in [0, 1]^2,$$
$$\psi(x, 0, t) = \psi(x, 1, t), \qquad \text{and} \qquad \psi(0, y, t) = \psi(1, y, t),$$

where $\boldsymbol{u} = (1, 1)$ is the advection velocity and the initial condition is given by

$$\psi(x, y, 0) = \frac{1}{4} \left(3 - \cos(2\pi x)\right) \left(3 - \cos(2\pi y)\right).$$

The square domain is divided into $2N^2$ triangular elements, and a global SBP operator is constructed using the assembly process described in Section C. The classical 4th-order Runge-Kutta scheme is used to time march the solution. For the results below, we define a nominal element size of $h = 1/N$.

Figure 2 shows the L^2-norm of the solution error versus element size after one period. For a given mesh size, the results show the expected qualitative benefit of using higher order discretizations. A similar benefit is observed when plotting accuracy versus CPU time [23]. We note that the $p = 2$ and $p = 4$ results have asymptotic convergence rates that are lower than expected; we do not have an explanation for this behavior at this time.

Next we demonstrate the stability properties of the multidimensional SBP operators. Figure 3 shows the spectra of the discretized spatial operator $\boldsymbol{u} \cdot \nabla$ for the SBP operators corresponding to $p = 1$ through $p = 4$ with $h = 1/12$. The spectra have essentially zero real part, which is consistent with the continuous spatial operator. For comparison, the figure also plots the spectra corresponding to the diagonal-mass matrix SE method. The SE operators' spectra have significant real parts.

The mimetic behaviour of the SBP spectra has practical implications. Figure 4 shows the change in the L^2 norm of the solution over two periods using the $p = 2$, $p = 3$ and $p = 4$ SBP discretizations and the corresponding SE discretizations[c]. The CFL number, defined as $\sqrt{2}\Delta t/h$, was fixed at 0.01 to ensure temporal errors were negligible relative to the spatial errors. The results clearly illustrate exponential growth in the

[c]The $p = 1$ SBP and SE discretizations are identical to one another and both are stable, so they are not included in the plot.

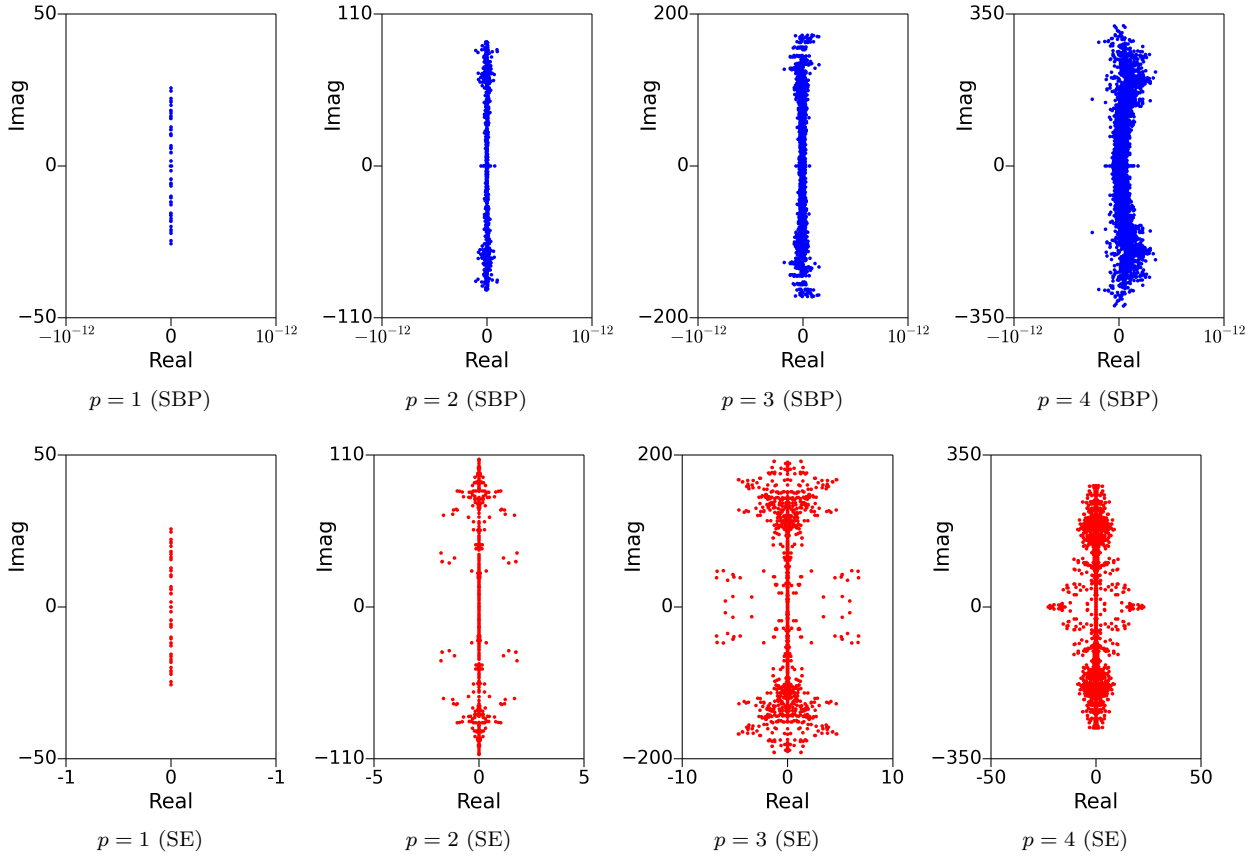

Figure 3. Eigenvalue distributions for the two discretizations of the linear convection problem: SBP (upper row) and the SE (lower row).

solution norm of the SE discretizations, while the SBP discretizations remain stable. The slight increase in the solution error of the $p = 2$ and $p = 3$ SBP results is due to temporal error that can be eliminated using a smaller CFL number.

IV. Summary and Discussion

When they proposed the classical SBP definition, Kreiss and Scherer [7] were seeking a finite-difference scheme that mimics integration-by-parts in the same way that finite-element methods do. Given this lineage, it should not be surprising to find that SBP operators share a significant amount in common with finite-element methods. Indeed, one can interpret an SBP operator as the result of applying the Galerkin finite-element method to a nominal basis that has no closed form expression.

Viewing SBP operators from the perspective of elements with implicit basis functions opens a number of avenues. In the case of generalized one-dimensional SBP operators, this perspective provides the flexibility to alter the nodal distribution to meet various criteria of interest. The element perspective also opens the door to multidimensional SBP operators defined on, for example, triangular or tetrahedral domains. Finally, by exploiting an analogy with the continuous Galerkin method, we demonstrated that SBP operators on a global domain can be assembled from elemental operators.

As discussed in the introduction, many different high-order discretizations have been proposed. What advantage do SBP operators offer over these other methods? While many existing methods offer accuracy, efficiency, and provable stability, we believe a significant advantage of the SBP framework is its flexibility, which enables a wide range of provably stable methods to be constructed with properties tailored to particular problem classes. The work described in this paper scratches the surface of this flexibility and many opportunities remain to be explored.

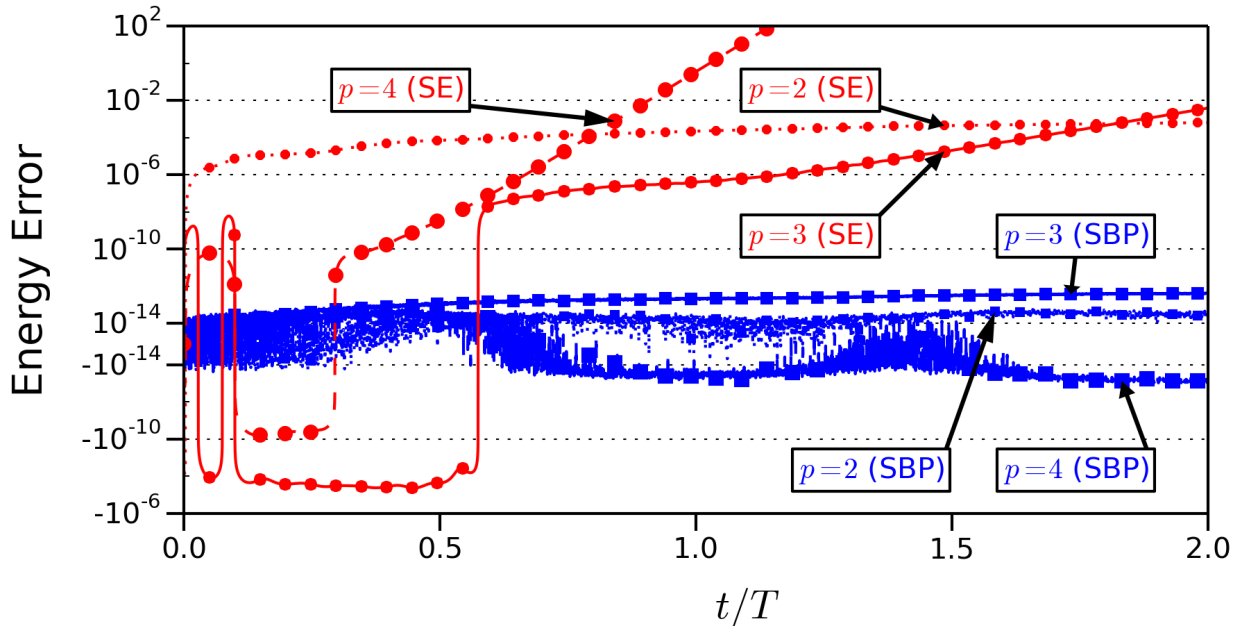

Figure 4. Change in the solution energy norm over two periods using SBP and SE discretizations for $p = 2$, $p = 3$ and $p = 4$. The $p = 1$ case is time-stable for both discretizations. Note the use of a symmetric logarithmic scale on the vertical axis.

References

[1]Kreiss, H.-O. and Oliger, J., "Comparison of accurate methods for the integration of hyperbolic equations," *Tellus*, Vol. 24, No. 3, 1972, pp. 199–215.

[2]Swartz, B. and Wendroff, B., "The relative efficiency of finite difference and finite element methods. I: Hyperbolic problems and splines," *SIAM Journal on Numerical Analysis*, Vol. 11, No. 5, 1974, pp. 979–993.

[3]Wang, Z. J., Fidkowski, K. J., Abgrall, R., Bassi, F., Caraeni, D., Cary, A., Deconinck, H., Hartmann, R., Hillewaert, K., Huynh, H. T., Kroll, N., Mayer, G., Persson, P.-O., van Leer, B., and Visbal, M., "High-order CFD methods: Current status and perspective," *International journal for numerical methods in fluids*, Vol. 72, No. 8, 2013, pp. 811–845.

[4]De Rango, S. and Zingg, D. W., "Higher-order spatial discretization for turbulent aerodynamic computations," *AIAA Journal*, Vol. 39, No. 7, 2001, pp. 1296–1304.

[5]Lomax, H., Pulliam, T. H., and Zingg, D. W., *Fundamentals of Computational Fluid Dynamics*, Springer-Verlag, 2001.

[6]Ditkowski, A., "High Order Finite Difference Schemes Whose Convergence Rates are Higher Then Their Truncation Errors," *ICOSAHOM*, 2015.

[7]Kreiss, H.-O. and Scherer, G., "Finite element and finite difference methods for hyperbolic partial differential equations," *Mathematical aspects of finite elements in partial differential equations*, Academic Press, New York/London, 1974, pp. 195–212.

[8]Strand, B., "Summation by parts for finite difference approximations for d/dx," *Journal of Computational Physics*, Vol. 110, No. 1, 1994, pp. 47–67.

[9]Svärd, M. and Nordström, J., "Review of summation-by-parts schemes for initial-boundary-value-problems," *Journal of Computational Physics*, Vol. 268, No. 1, 2014, pp. 17–38.

[10]Del Rey Fernández, D. C., Hicken, J. E., and Zingg, D. W., "Review of summation-by-parts operators with simultaneous approximation terms for the numerical solution of partial differential equations," *Computers & Fluids*, Vol. 95, No. 22, 2014, pp. 171–196.

[11]Carpenter, M. H., Gottlieb, D., and Abarbanel, S., "Time-stable boundary conditions for finite-difference schemes solving hyperbolic systems: Methodology and application to high-order compact schemes," *Journal of Computational Physics*, Vol. 111, No. 2, 1994, pp. 220–236.

[12]Nordström, J., Gong, J., van der Weide, E., and Svärd, M., "A stable and conservative high order multi-block method for the compressible Navier-Stokes equations," *Journal of Computational Physics*, Vol. 228, No. 24, 2009, pp. 9020–9035.

[13]Carpenter, M. H., Nordström, J., and Gottlieb, D., "Revisiting and Extending Interface Penalties for Multi-domain Summation-by-Parts Operators," *Journal of Scientific Computing*, Vol. 45, No. 1-3, 2010, pp. 118–150.

[14]Carpenter, M. H. and Gottlieb, D., "Spectral methods on arbitrary grids," *Journal of Computational Physics*, Vol. 129, No. 1, 1996, pp. 74–86.

[15]Gassner, G. J., "A skew-symmetric discontinuous Galerkin spectral element discretization and its relation to SBP-SAT finite difference methods," *SIAm Journal on Scientific Computing*, Vol. 35, No. 3, 2013, pp. A1233–A1253.

[16]Del Rey Fernández, D. C., Boom, P. D., and Zingg, D. W., "A Generalized Framework for Nodal First Derivative Summation-By-Parts Operators," *Journal of Computational Physics*, Vol. 266, No. 1, 2014, pp. 214–239.

[17]Hicken, J. E. and Zingg, D. W., "Dual consistency and functional accuracy: a finite-difference perspective," *Journal of Computational Physics*, Vol. 256, Jan. 2014, pp. 161–182.

[18]Del Rey Fernández, D. C., *Generalized summation-by-parts operators for first and second derivatives*, Ph.D. thesis, University of Toronto Institute for Aerospace Studies, 4925 Dufferin Street, Toronto, Ontario, Canada M3H 5T6, 2015.

[19]Alpert, B. K., "Hybrid Gauss-trapezoidal quadrature rules," *SIAM Journal on Scientific Computing*, Vol. 5, 1999, pp. 1551–1584.

[20]Del Rey Fernández, D. C. and Zingg, D. W., "New diagonal-norm summation-by-parts operators for the first derivative with increased order of accuracy," *AIAA aviation 2015*, 2015.

[21]Del Rey Fernández, D. C. and Zingg, D. W., "Generalized summation-by-parts operators for the second derivative with a variable coefficient," *Submitted to SIAM Journal on Scientific Computing, (see arXiv:1410.0201[Math.NA])*, 2014.

[22]Mattsson, K., Almquist, M., and Carpenter, M. H., "Optimal diagonal-norm SBP operators," *Journal of Computational Physics*, Vol. 264, No. 1, 2014, pp. 91–111.

[23]Hicken, J. E., Del Rey Fernández, D. C., and Zingg, D. W., "Multidimensional Summation-By-Parts Operators: General Theory and Application to Simplex Elements," May 2015, submitted to the Journal of Computational Physics (see also http://arxiv.org/abs/1505.03125).

[24]Hicken, J. E. and Zingg, D. W., "Summation-by-parts operators and high-order quadrature," *Journal of Computational and Applied Mathematics*, Vol. 237, No. 1, 2013, pp. 111–125.

[25]Kwan-yu Chiu, E., Wang, Q., Hu, R., and Jameson, A., "A Conservative Mesh-Free Scheme and Generalized Framework for Conservation Laws," *SIAM Journal on Scientific Computing*, Vol. 34, No. 6, Jan. 2012, pp. A2896–A2916.

[26]Chiu, E. K., Wang, Q., and Jameson, A., "A conservative meshless scheme: general order formulation and application to Euler equations," *49th AIAA Aerospace Sciences Meeting*, No. AIAA–2011–651, Orlando, Florida, Jan. 2011.

[27]Kitson, A., McLachlan, R. I., and Robidoux, N., "Skew-adjoint finite difference methods on nonuniform grids," *New Zealand Journal of Mathematics*, Vol. 32, No. 2, 2003, pp. 139–159.

[28]Liu, Y. and Vinokur, M., "Exact Integrations of Polynomials and Symmetric Quadrature Formulas over Arbitrary Polyhedral Grids," *Journal of Computational Physics*, Vol. 140, No. 1, 1998, pp. 122–147.

[29]Cohen, G., Joly, P., Roberts, J. E., and Tordjman, N., "Higher Order Triangular Finite Elements with Mass Lumping for the Wave Equation," *SIAM Journal on Numerical Analysis*, Vol. 38, No. 6, Jan. 2001, pp. 2047–2078.

[30]Mulder, W. A., "Higher-order mass-lumped finite elements for the wave equation," *Journal of Computational Acoustics*, Vol. 09, No. 02, June 2001, pp. 671–680.

[31]Giraldo, F. X. and Taylor, M. A., "A diagonal-mass-matrix triangular-spectral-element method based on cubature points," *Journal of Engineering Mathematics*, Vol. 56, No. 3, 2006, pp. 307–322.

[32]Zhang, L., Cui, T., and Liu, H., "A Set of Symmetric Quadrature Rules on Triangles and Tetrahedra," *Journal of Computational Mathematics*, Vol. 27, No. 1, 2009, pp. 89–96.

[33]Witherden, F. D. and Vincent, P. E., "On the Identification of Symmetric Quadrature Rules for Finite Element Methods," Sept. 2014, http://arxiv.org/abs/1409.1865.

[34]Hesthaven, J. S. and Warburton, T., *Nodal discontinuous Galerkin methods: algorithms, analysis, and applications*, Springer-Verlag, New York, 2008.

[35]Golub, G. H. and Van Loan, C. F., *Matrix Computations*, The John Hopkins University Press, 3rd ed., 1996.

[36]Liu, Y., Vinokur, M., and Wang, Z. J., "Spectral difference method for unstructured grids I: Basic formulation," *Journal of Computational Physics*, Vol. 216, No. 2, Aug. 2006, pp. 780–801.